

Monolithic Finite Element Methods for the simulation of thixo-viscoplastic flows

N. Begum, A. Ouazzi, S. Turek
Institute of Applied Mathematics, LS III,
TU Dortmund University, Dortmund, Germany

6th ECCOMAS Young Investigators Conference YIC2021
7-9 July 2021, Valencia Spain

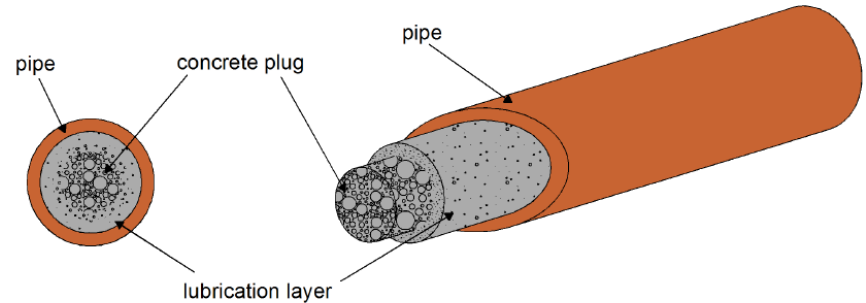
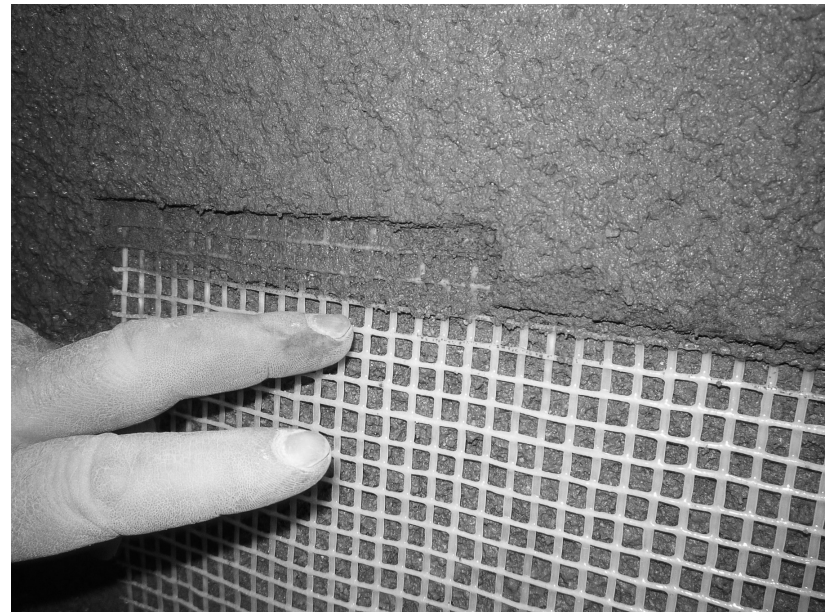


Why “Thixotropic materials?

- Processing of thixotropic materials relevant for industrial applications
 - ➔ Lubrication, asphalt, self-compacting concrete...
- Physically fascinating due to improved mechanical properties

Goal:

- Modern CFD methods with high accuracy, robustness and efficiency for thixotropic materials
 - ➔ Saving time, money and resources



Investigation of solid/liquid and liquid/solid transitions based on micro-structure

- Thixotropy means
 - combination of two greek words
 - Thixis: shaking/stirring
 - trepo: turning/changing
- Thixotropy concept
 - Based on viscosity
 - Flow induced by time-dependent decrease of viscosity
 - The phenomena is reversible
- Rejuvenation / Breakdown
 - “Faster” flow: fluid rejuvenates
 - Decreases of viscosity with acceleration of the flow
- Aging / Build-up
 - At rest or under slow flow: fluid ages
 - Increases of the viscosity in time



HPC features:

- Moderately parallel
- GPU computing
- Open source



Hardware-oriented Numerics

Numerical features:

- Higher order **FEM** in space & (semi-) **Implicit** FD/FEM in time
- Semi-(un)structured meshes with dynamic **adaptive grid** deformation
- Fictitious Boundary (FBM) methods
- **Newton-Multigrid**-type solvers

Non-Newtonian flow module:

- generalized Newtonian model (Power-law, Carreau, Houska,...)
- viscoelastic differential model (Giesekus, FENE, Oldroyd,...)

Multiphase flow module (resolved interfaces):

- l/l – interface capturing (Level Set)
- s/l – interface tracking (FBM)
- s/l/l – combination of l/l and s/l

Engineering aspects:

- Geometrical design
- Modulation strategy
- Optimization

Here: FEM-based tools for the accurate simulation of (thixotropic) flow problems, particularly with complex rheology



For details, please visit: www.featflow.de

→ starting point: Generalized Navier-Stokes equations (+initial and boundary conditions)

$$\rho \left(\frac{\partial}{\partial t} + \mathbf{u} \cdot \nabla \right) \mathbf{u} - \nabla \cdot \boldsymbol{\sigma} + \nabla p = \rho f,$$
$$\nabla \cdot \mathbf{u} = 0,$$

- velocity- and pressure field \mathbf{u} and p
- stress tensor $\boldsymbol{\sigma}$
- linear material behaviour - Newtonian fluids

$$\boldsymbol{\sigma} = 2\eta_s \mathbf{D}(\mathbf{u}) \quad : \eta_s \text{ is constant viscosity}$$

- non-linear material behaviour- structurally viscous / viscoplastic

$$\boldsymbol{\sigma} = 2\eta_s(D_{\mathbb{II}}, p, \Theta, \lambda) \mathbf{D}(\mathbf{u}), \quad D_{\mathbb{II}} = \text{tr} \left(\frac{1}{2} \mathbf{D}(\mathbf{u})^2 \right)$$


- Power-law, Carreau, Bingham, Herschel-Bulkley, Houska, ...

- structure parameter λ

- Archetypical thixotropic viscoplastic (TVP) models

$$\begin{cases} \sigma = 2\eta(D_{\text{II}}, \lambda)\mathbf{D}(\mathbf{u}) + \sqrt{2}\tau(\lambda)\frac{\mathbf{D}(\mathbf{u})}{\sqrt{D_{\text{II}}}} & \text{if } D_{\text{II}} \neq 0 \\ \sigma_{\text{II}} \leq \tau(\lambda) & \text{if } D_{\text{II}} = 0 \end{cases}$$

- Relations between rheological parameters and structural parameter

	$\eta(D_{\text{II}}, \lambda)$	$\tau(\lambda)$
Worrall and Tulliani ¹	$\lambda\eta_0$	τ_0
Coussot <i>et al.</i> ²	$\lambda^a\eta_0$	—
Houska ³	$(\eta_0 + \eta_1\lambda)D_{\text{II}}^{\frac{(n-1)}{2}}$	$(\tau_0 + \tau_1\lambda)$
Mujumbar <i>et al.</i> ⁴	$(\eta_0 + \eta_1\lambda)D_{\text{II}}^{\frac{(n-1)}{2}}$	$\lambda^{a+1}G_0\Lambda_c^*$
Burgos <i>et al.</i> ⁵	η_0	$\lambda\tau_0$
Dullaert & Mewis ⁶	$\lambda\eta_0$	$\lambda G_0 \left(\lambda D_{\text{II}}^{\frac{1}{2}} \right) \Lambda_c^*$

* Λ_c is a constant/variable elastic strain.



- General format of evolution equation for structural parameter:

$$\frac{\partial \lambda}{\partial t} + u \cdot \nabla \lambda = F_{buildup} - F_{breakdown}$$

- Expressions for different thixotropic models:

	$F_{buildup}$	$F_{breakdown}$
Worrall and Tulliani ¹	$c_1(1 - \lambda)D_{II}^{\frac{1}{2}}$	$c_2\lambda D_{II}^{\frac{1}{2}}$
Coussot <i>et al.</i> ²	c_1	$c_2\lambda D_{II}^{\frac{1}{2}}$
Houska ³	$c_1(1 - \lambda)$	$c_2\lambda^m D_{II}^{\frac{1}{2}}$
Mujumbar <i>et al.</i> ⁴	$c_1(1 - \lambda)$	$c_2\lambda D_{II}^{\frac{1}{2}}$
Burgos <i>et al.</i> ⁵	$c_1(1 - \lambda)$	$c_2\lambda D_{II}^{\frac{1}{2}} \exp(aD_{II}^{\frac{1}{2}})$
Dullaert & Mewis ⁶	$(c_1 + c_3 D_{II}^{\frac{1}{2}})(1 - \lambda)t^{-b}$	$c_2\lambda D_{II}^{\frac{1}{2}}t^{-b}$

- **Viscoplastic (VP) flow**

$$\begin{cases} \boldsymbol{\sigma} = 2\eta_0 \mathbf{D}(\mathbf{u}) + \sqrt{2}\tau_0 \frac{\mathbf{D}(\mathbf{u})}{\sqrt{D_{\text{II}}}} & \text{if } D_{\text{II}} \neq 0 \\ \sigma_{\text{II}} \leq \tau_0 & \text{if } D_{\text{II}} = 0 \end{cases}$$

- **Thixo-viscoplastic (TVP) flow**

$$\begin{cases} \boldsymbol{\sigma} = 2\eta(D_{\text{II}}, \lambda) \mathbf{D}(\mathbf{u}) + \sqrt{2}\tau(\lambda) \frac{\mathbf{D}(\mathbf{u})}{\sqrt{D_{\text{II}}}} & \text{if } D_{\text{II}} \neq 0 \\ \sigma_{\text{II}} \leq \tau(\lambda) & \text{if } D_{\text{II}} = 0 \end{cases}$$

→ **Affine functions**

$$\begin{cases} \eta(\lambda) = \eta_0 + \eta_1 \lambda \\ \tau(\lambda) = \tau_0 + \tau_1 \lambda \end{cases}$$

→ **Structure evolution equation**

$$\frac{\partial \lambda}{\partial t} + \mathbf{u} \cdot \nabla \lambda = a(1 - \lambda) - b\lambda D_{\text{II}}^{\frac{1}{2}}$$

(a, b are structure parameters)

- **Viscosity model for TVP flow i.e. extended viscosity defined on all domains s.t.**

$$\left\{ \begin{array}{ll} I. & \eta_s(D_{\mathbb{II}}, \lambda) = \eta(\lambda) + \frac{\sqrt{2}}{2} \tau(\lambda) \frac{1}{\sqrt{(D_{\mathbb{II}} + (k^{-1})^2)}} \\ II. & \eta_s(D_{\mathbb{II}}, \lambda) = \eta(\lambda) + \frac{\sqrt{2}}{2} \tau(\lambda) \frac{1}{D_{\mathbb{II}}^{\frac{1}{2}}} (1 - e^{-k D_{\mathbb{II}}^{\frac{1}{2}}}) \end{array} \right. \\ (k : \text{ regularization parameter})$$

- **Full set of equations**

$$\left\{ \begin{array}{ll} \left(\frac{\partial}{\partial t} + u \cdot \nabla \right) u - \nabla \cdot \left(2\eta_s(D_{\mathbb{II}}, \lambda) D(u) \right) + \nabla p = 0 & \text{in } \Omega \\ \nabla \cdot u = 0 & \text{in } \Omega \\ \frac{\partial \lambda}{\partial t} + u \cdot \nabla \lambda - a(1 - \lambda) + b\lambda D_{\mathbb{II}}^{\frac{1}{2}} = 0 & \text{in } \Omega \end{array} \right.$$

Let $\mathcal{U} = (\lambda, \mathbf{u}, p)$, and $\mathcal{R}_{\mathcal{U}}(\mathcal{U})$ be the continuous or the discrete corresponding system's residuum.

- Update of the nonlinear iteration with the correction $\delta\mathcal{U}$ i.e.

$$\mathcal{U}^N = \mathcal{U} + \delta\mathcal{U}$$

- The linearization of the residual provides

$$\begin{aligned}\mathcal{R}_{\mathcal{U}}(\mathcal{U}^N) &= \mathcal{R}_{\mathcal{U}}(\mathcal{U} + \delta\mathcal{U}) \\ &= \mathcal{R}_{\mathcal{U}}(\mathcal{U}) + \mathcal{J}(\mathcal{U}) \cdot \delta\mathcal{U}\end{aligned}$$

- The Newton's method assuming invertible Jacobian

$$\mathcal{U}^N = \mathcal{U} - \mathcal{J}^{-1}(\mathcal{U}) \mathcal{R}_{\mathcal{U}}(\mathcal{U})$$



Jacobian calculations

$$\mathcal{J}(\mathcal{U}) = \left(\frac{\partial \mathcal{R}_u(\mathcal{U})}{\partial \mathcal{U}} \right)$$

- Continuous Adaptive Newton based on a priori study of Jacobian's properties and decompositions

$$\mathcal{J}(\mathcal{U}) = \left(\frac{\partial \hat{\mathcal{R}}_u(\mathcal{U})}{\partial \mathcal{U}} \right) + \delta \left(\frac{\partial \tilde{\mathcal{R}}_u(\mathcal{U})}{\partial \mathcal{U}} \right)$$

- Discrete Adaptive Newton based on the rate of residum's convergence

$$\left(\frac{\partial \mathcal{R}}{\partial \mathcal{U}} \right)_{ij} \approx \left(\frac{\mathcal{R}_i(\mathcal{U} + \epsilon e_j) - \mathcal{R}_i(\mathcal{U} - \epsilon e_j)}{2\epsilon} \right)$$



- **Flow variables** (λ, \mathbf{u}, p)

- **Set** $\mathbb{T} := L^2(\Omega), \mathbb{V} := [H_0^1(\Omega)]^2, \mathbb{Q} := L_0^2(\Omega)$
- **Set** $\tilde{\mathbf{u}} := (\lambda, \mathbf{u})$
- **Find** $(\lambda, \mathbf{u}, p) \in (\mathbb{T} \cap H^1(\Omega)) \times \mathbb{V} \times \mathbb{Q}$ **s.t.**

$$\langle \mathcal{K}(\lambda, \mathbf{u}, p), (\xi, \mathbf{v}, q) \rangle = \langle \mathcal{L}, (\xi, \mathbf{v}, q) \rangle, \quad \forall (\xi, \mathbf{v}, q) \in \mathbb{T} \times \mathbb{V} \times \mathbb{Q}$$

$$\mathcal{K} = \begin{bmatrix} \mathcal{A}_{\tilde{\mathbf{u}}} & \mathcal{B}^T \\ \mathcal{B} & 0 \end{bmatrix}$$

- **Compatibility constraints**

$$\sup_{\mathbf{v} \in \mathbb{V}} \frac{\langle \mathcal{B}\mathbf{v}, q \rangle}{\|\mathbf{v}\|_{\mathbb{V}}} \geq \beta \|q\|_{\mathbb{Q}/\text{Ker } \mathcal{B}^T}, \quad \forall q \in \mathbb{Q}$$



- Discretizations have to handle the following challenges

- Stable FEM spaces
- Non-symmetric, non-coercive and ill-posedness
- Convection and positivity preserving
- Locally adapted meshes for steep gradients

- Solvers have to deal with

- Different source of nonlinearities
- Strong coupling of equations
- Robustness and efficiency

- **Conforming approximations**

$$\mathbb{T}_h \subset \mathbb{T}, \quad \mathbb{V}_h \subset \mathbb{V}, \quad \mathbb{Q}_h \subset \mathbb{Q}$$

$$\mathcal{A}_{\tilde{\mathbf{u}}_h} = \mathcal{A}_{\tilde{\mathbf{u}}}, \mathcal{B}_h = \mathcal{B}$$

- **Discrete inf-sup condition**

$$\sup_{\mathbf{v}_h \in \mathbb{V}_h} \frac{\langle \mathcal{B}_h \mathbf{v}_h, q_h \rangle}{\|\mathbf{v}_h\|_{\tilde{\mathbb{V}}}} \geq \beta_h \|q_h\|_{\mathbb{Q}/Ker \mathcal{B}_h^T}, \quad \forall q_h \in \mathbb{Q}_h$$

The family of conforming FEM $Q_r/Q_r/P_{r-1}^{\text{disc}}$, $r \geq 2$ **for** (λ, \mathbf{u}, p) **with stabilization**

$$J_u(u_h, v_h) = \gamma_u \sum_{e \in \mathcal{E}_h} h^2 \int_e [\nabla u_h] : [\nabla v_h] d\Omega$$

$$J_\lambda(\lambda_h, \xi_h) = \gamma_\lambda \sum_{e \in \mathcal{E}_h} h \int_e [\nabla \lambda_h] : [\nabla \xi_h] d\Omega$$

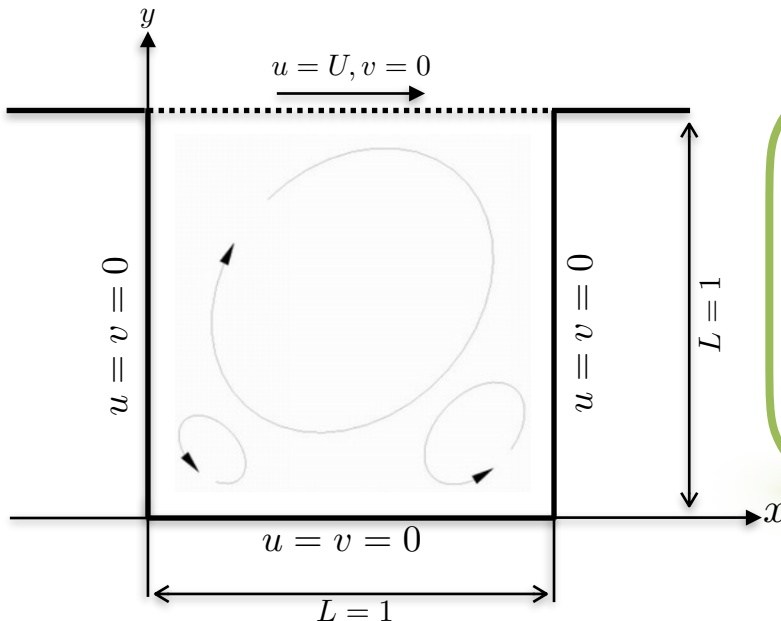
- Inf-sup conditions is satisfied
- Discontinuous pressure
 - Good for the solver
 - Element-wise mass conservation
- Discrete problem is well-posed
- Highly consistent and symmetric stabilization
- Robust solver w.r.t. the monolithic approach
- Efficient solver w.r.t. multigrid solver

- Standard geometric multigrid solver for linearized system
- Full Q_r and P_{r-1}^{disc} restriction and prolongation
- Local Multilevel Pressure Schur Complement via Vanka-like smoother

$$\begin{pmatrix} \lambda^{l+1} \\ u^{l+1} \\ p^{l+1} \end{pmatrix} = \begin{pmatrix} \lambda^l \\ u^l \\ p^l \end{pmatrix} + \omega^l \sum_{T \in \mathcal{T}_h} \left((\mathcal{K}_h + \mathcal{J})|_T \right)^{-1} \begin{pmatrix} \mathcal{R}_{\lambda^l} \\ \mathcal{R}_{u^l} \\ \mathcal{R}_{p^l} \end{pmatrix}|_T$$

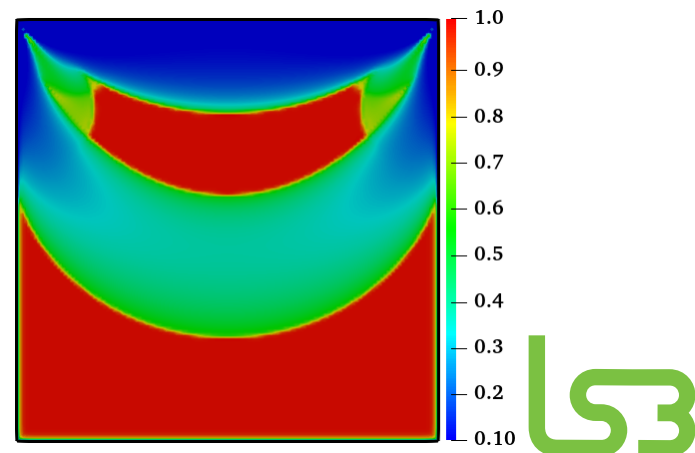
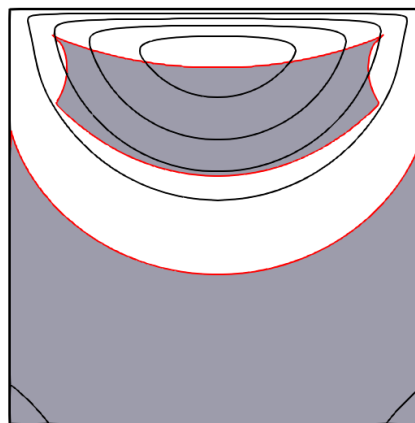
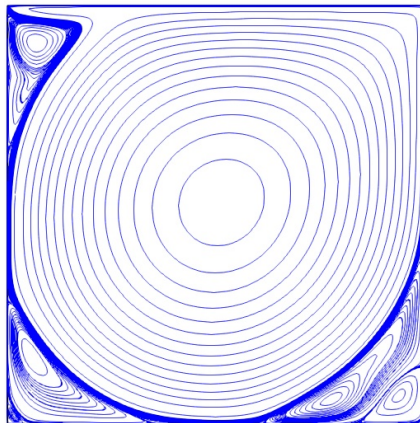
Coupled Monolithic Multigrid Solver !



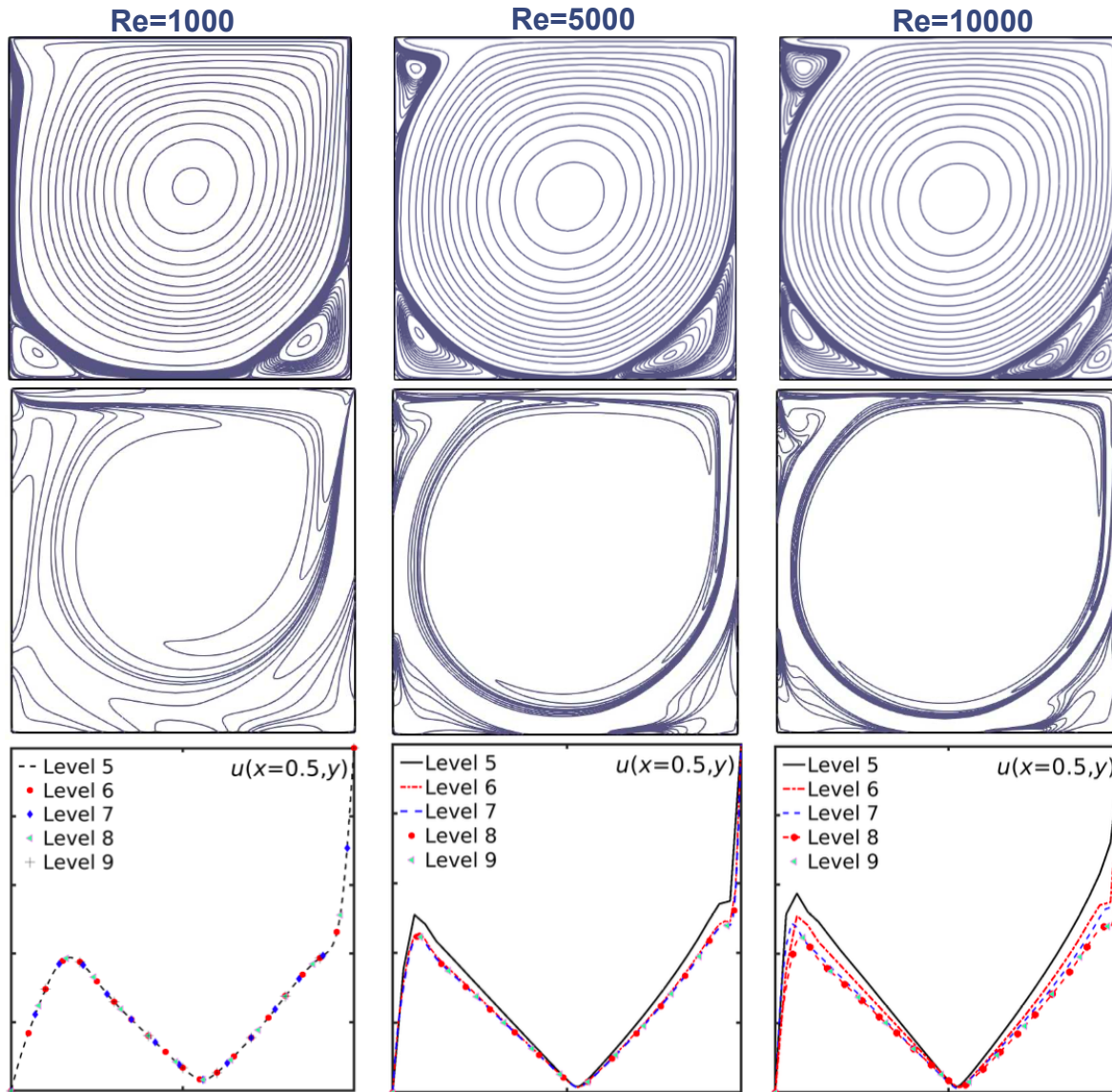


- ▶ Starting point: consider flow in a cavity with unit height
- ▶ Steady, incompressible flow
- ▶ Constant speed at upper lid
- ▶ No-slip Dirichlet boundary conditions

▶ Newtonian, Viscoplastic, and Thixo-viscoplastic (TVP)



- Point-wise convergence for Newtonian flow



- Global and point-wise quantities and solver behaviour

Re	Level	1000		5000		10000	
		cells	Energy $\times 10^2$	N/M	Energy $\times 10^2$	N/M	Energy $\times 10^2$
5	1024	4.541506	5/1	6.082524	6/1	7.940472	7/1
6	4096	4.458877	5/1	4.955858	5/1	5.369527	6/1
7	16384	4.452357	3/1	4.768669	4/1	4.868399	5/1
8	65536	4.451904	3/1	4.744815	3/2	4.783917	4/2
9	262144	4.451846	3/1	4.742921	3/1	4.773500	3/2
10	1048576	4.451834	2/1	4.742815	3/1	4.772692	3/1
<i>Ref. values</i> ≈:		4.45		4.74		4.77	

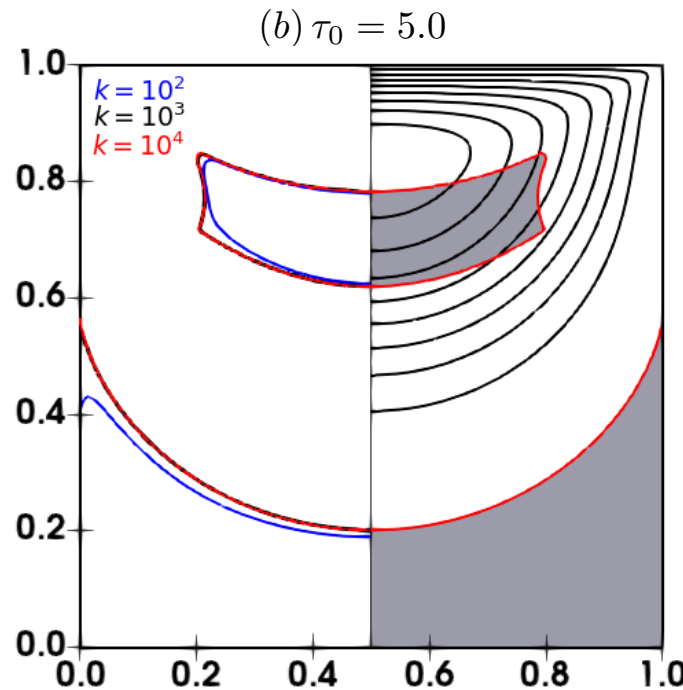
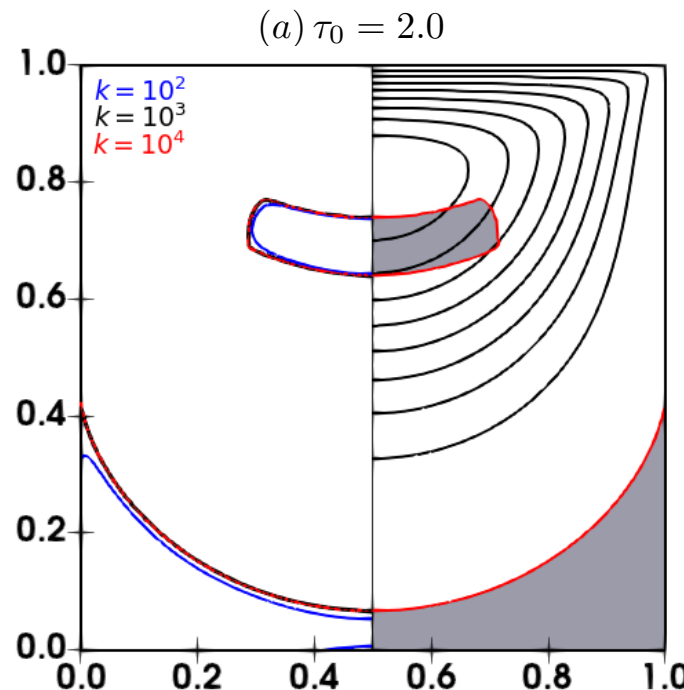
Re	1000		5000		10000	
	Level	Ψ_{max}	$\Psi_{min} \times 10^3$	Level	Ψ_{max}	$\Psi_{min} \times 10^3$
6	0.1190073	-1.72813	0.1249471	-3.145666	0.1586626	-5.7535749
7	0.1189360	-1.72649	0.1225439	-3.077555	0.1236127	-3.2070181
8	0.1189361	-1.72851	0.1222499	-3.072411	0.1225210	-3.1831353
9	0.1189362	-1.72963	0.1222269	-3.073524	0.1224097	-3.1910101
10	0.1189366	-1.72965	0.1222259	-3.073589	0.1223892	-3.1797390
Ref.	0.11892	-1.7292	0.12216	-3.0706		
	Brunau	Bruneau	Kupperman	Bruneau		

- ✓ Mesh convergence of the solutions irrespective of Re number
- ✓ Efficient non-linear solver
- ✓ Mesh independent linear solver

Accurate, robust and efficient Monolithic Multigrid Solver



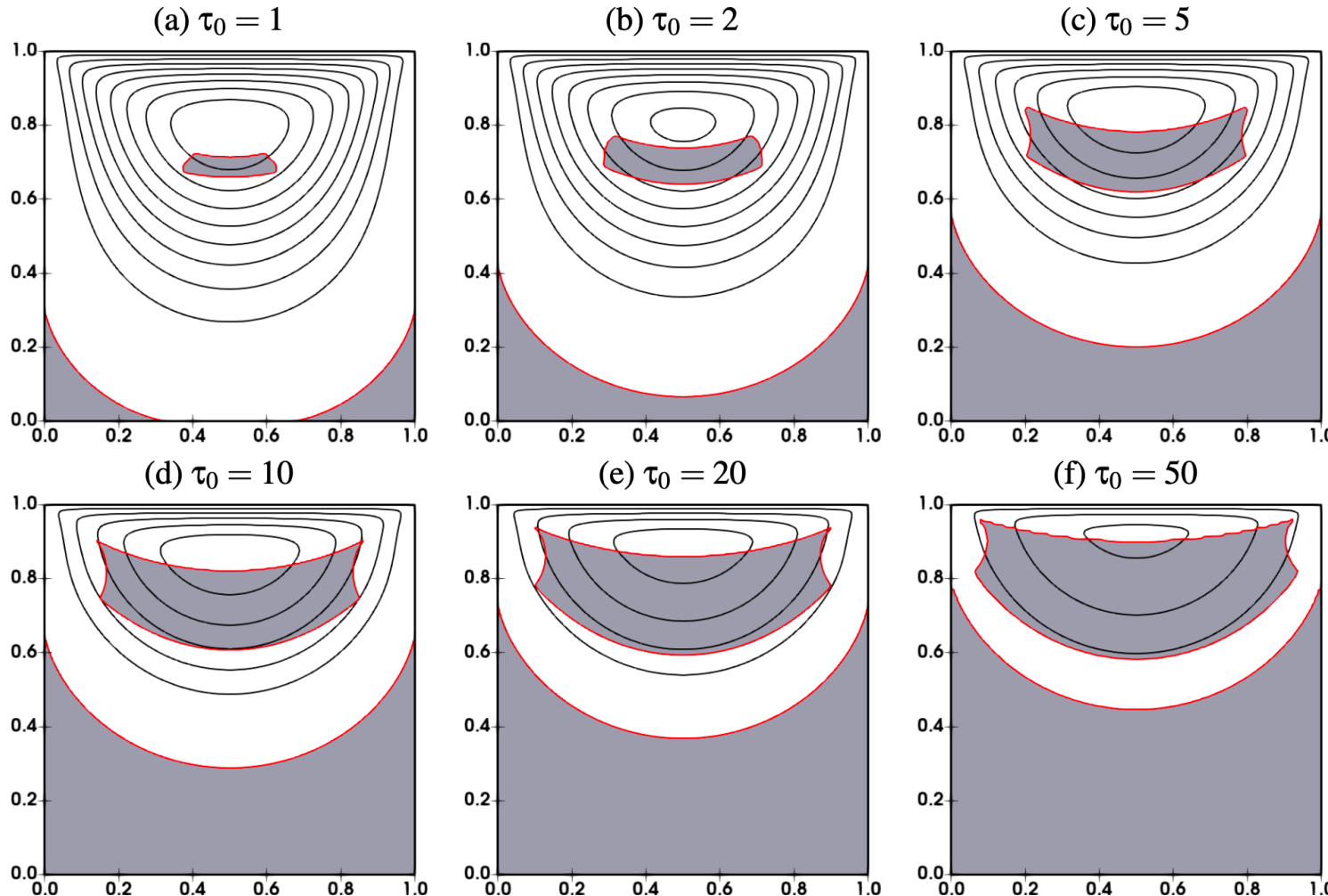
- Boundary limit for rigid-zone w.r.t regularization k



- Accurate track of interface requires
 - ✓ larger k solutions
 - ✓ finer mesh refinement
- Existence of pair (k, L) beyond which no further improvement in solutions is expected

Viscoplastic flow in Lid-driven cavity

- progressive growth of unyielded zones for non-thixotropic (Bingham Plastic) flow



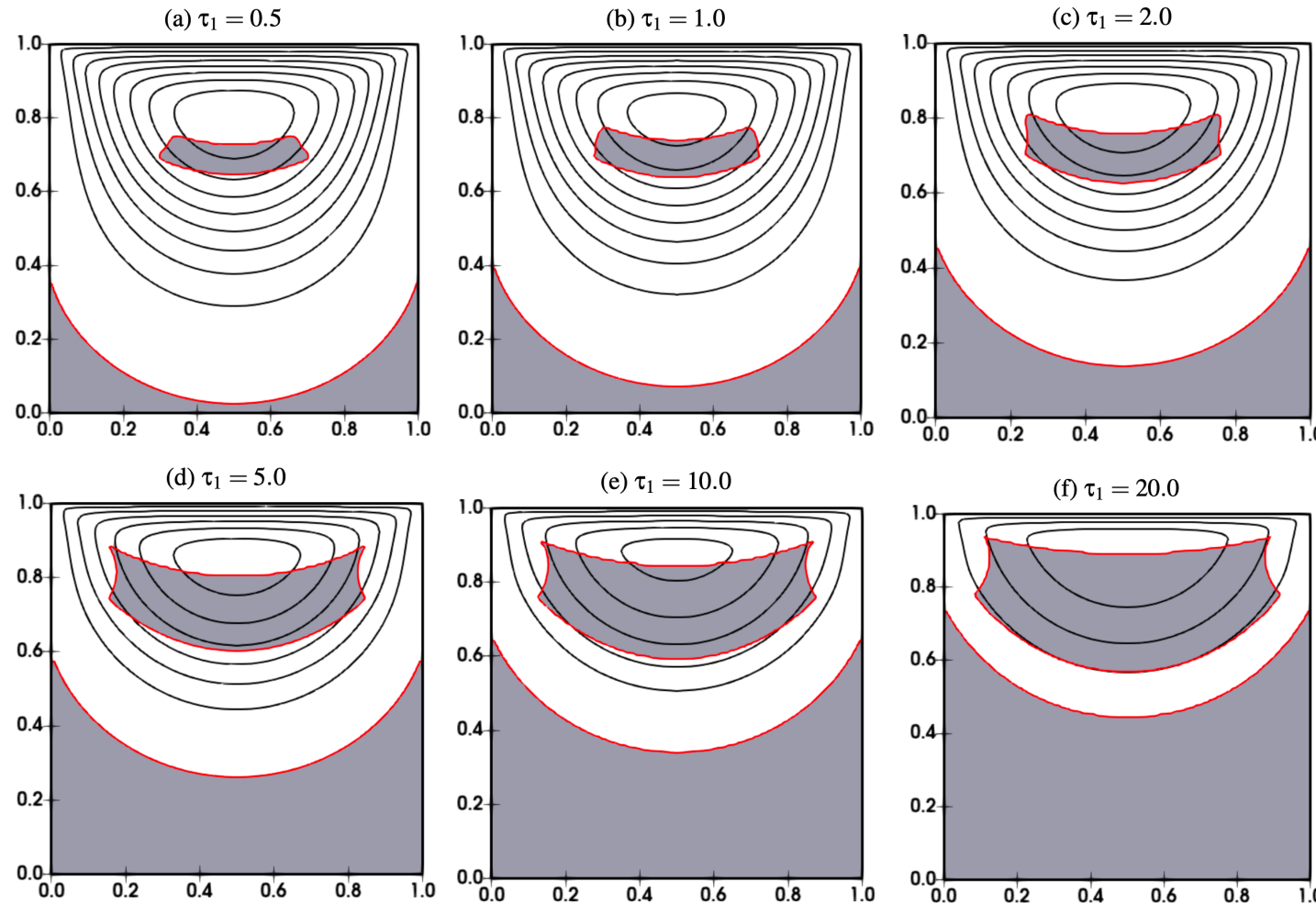
✓ Unyielded zones's shape and extent is in agreement with Ref. Results

- Solver behaviour w.r.t Regularization and mesh refinement

$k \backslash L$	5	6	7	5	6	7	5	6	7	
$\tau_0 = 1$					$\tau_0 = 2$			$\tau_0 = 5$		
1×10^1	3/1	3/1	3/1	3/1	3/1	3/1	4/1	4/1	4/1	
5×10^1	2/1	2/1	2/1	2/1	2/1	2/1	3/1	3/1	3/1	
1×10^2	3/1	3/1	3/1	3/1	3/1	3/1	4/1	4/1	4/1	
5×10^2	3/1	2/1	2/1	3/1	2/1	3/1	3/2	3/2	3/1	
1×10^3	2/2	3/2	3/1	3/1	3/1	4/1	4/1	5/2	5/2	
5×10^3	2/1	2/1	4/1	3/1	3/2	6/2	4/1	8/2	6/1	
1×10^4	2/1	2/2	5/1	3/1	3/1	6/1	4/1	5/4	6/3	
$\tau_0 = 10$					$\tau_0 = 20$			$\tau_0 = 50$		
1×10^1	5/1	5/1	5/1	6/1	6/1	6/1	5/1	7/1	7/1	
5×10^1	4/1	3/1	3/1	4/1	4/1	3/2	5/4	4/2	4/2	
1×10^2	5/2	4/1	4/1	5/2	5/2	5/1	6/5	5/4	5/1	
5×10^2	5/3	3/2	3/1	4/4	3/4	4/3	5/4	4/2	4/3	
1×10^3	5/2	7/4	9/1	5/5	7/2	8/1	5/5	9/2	9/2	
5×10^3	5/1	7/3	8/2	6/3	6/4	6/4	6/4	7/2	8/2	
1×10^4	6/1	7/2	8/3	6/3	5/5	7/3	6/3	7/3	8/2	

- ✓ Efficient non-linear solver
- ✓ Mesh independent linear solver
- ✓ Solutions are obtained with continuation strategy w.r.t. k
- Integration of continuation strategy w.r.t. k in the solver

- Impact of thixotropic yield stress on morphology of unyielded zones in TVP flow



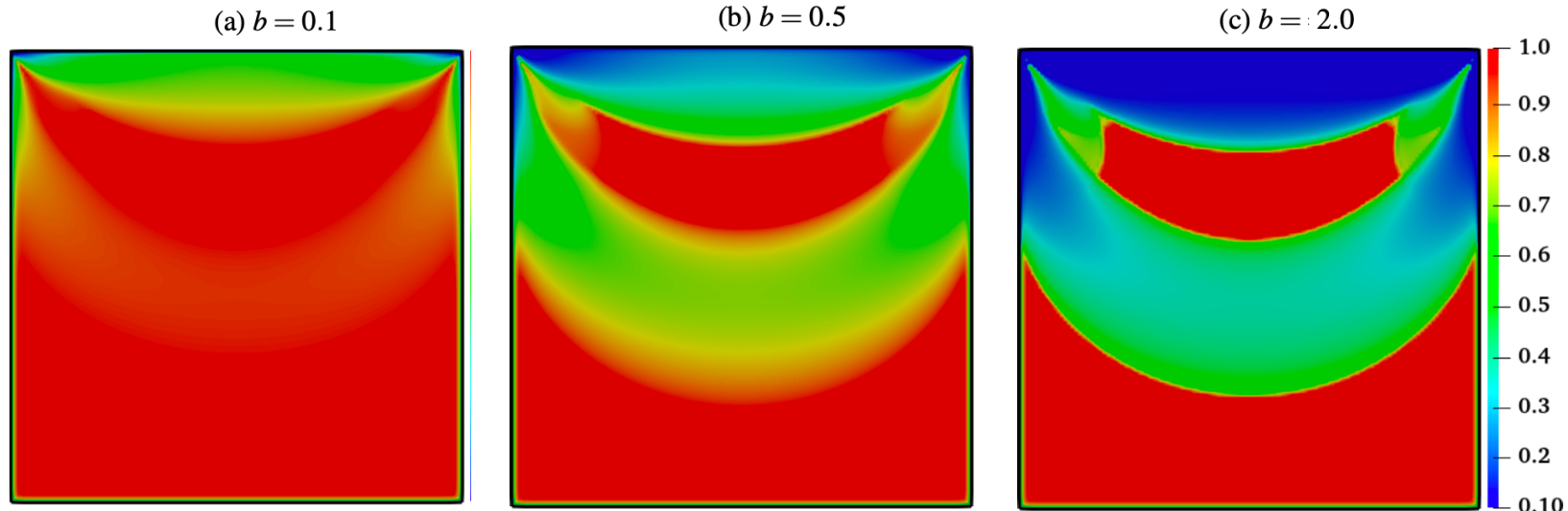
- ✓ Main rheological characteristics of materials with yield stress is preserved

- Solver behaviour w.r.t Regularization and mesh refinement

$k \setminus L$	5	6	7	5	6	7	5	6	7	
$\tau_1 = 0.5$					$\tau_1 = 1$			$\tau_1 = 2$		
1×10^1	5/2	5/3	6/2	5/2	5/2	9/1	5/2	5/2	9/1	
5×10^1	4/2	4/2	4/2	3/2	3/3	7/1	3/2	3/3	8/1	
1×10^2	4/1	4/2	5/1	4/1	4/2	7/1	4/2	4/2	8/1	
5×10^2	4/1	4/1	5/1	3/1	4/1	6/1	4/2	4/2	8/1	
1×10^3	4/1	4/1	4/1	4/2	4/2	8/1	4/4	6/1	7/1	
5×10^3	4/1	4/1	3/2	7/1	9/1	5/1	6/1	9/1	8/1	
1×10^4	4/1	4/2	4/2	5/1	7/1	4/1	7/1	10/1	8/2	
$\tau_1 = 5.0$					$\tau_1 = 10.0$			$\tau_1 = 20.0$		
1×10^1	6/2	6/2	10/1	11/1	8/2	11/1	10/1	9/2	11/1	
5×10^1	4/2	3/2	11/1	11/1	4/2	7/1	12/1	5/3	9/1	
1×10^2	4/2	5/2	11/1	10/1	5/3	8/1	12/1	6/3	10/1	
5×10^2	5/2	4/2	10/1	9/1	5/3	5/1	8/1	5/5	11/1	
1×10^3	5/2	9/1	10/1	10/1	9/1	7/1	8/2	9/1	9/2	
5×10^3	5/1	5/1	5/1	8/1	8/2	6/1	8/1	7/1	11/1	
1×10^4	5/1	5/2	5/1	8/3	7/1	5/1	8/2	7/1	9/1	

- ✓ Efficient non-linear solver
- ✓ Mesh independent linear solver
- ✓ Solutions are obtained with continuation strategy w.r.t. k
- Integration of continuation strategy w.r.t. k in the solver

- Material micro-structural level w.r.t. breakdown parameter



- Interplay of yield stress and thixotropy

- ✓ Structuring level is predicting shape and extent of rigid zones
- ✓ Induction of more breakdown layers
- ✓ Shear localization
- ✓ Shear band

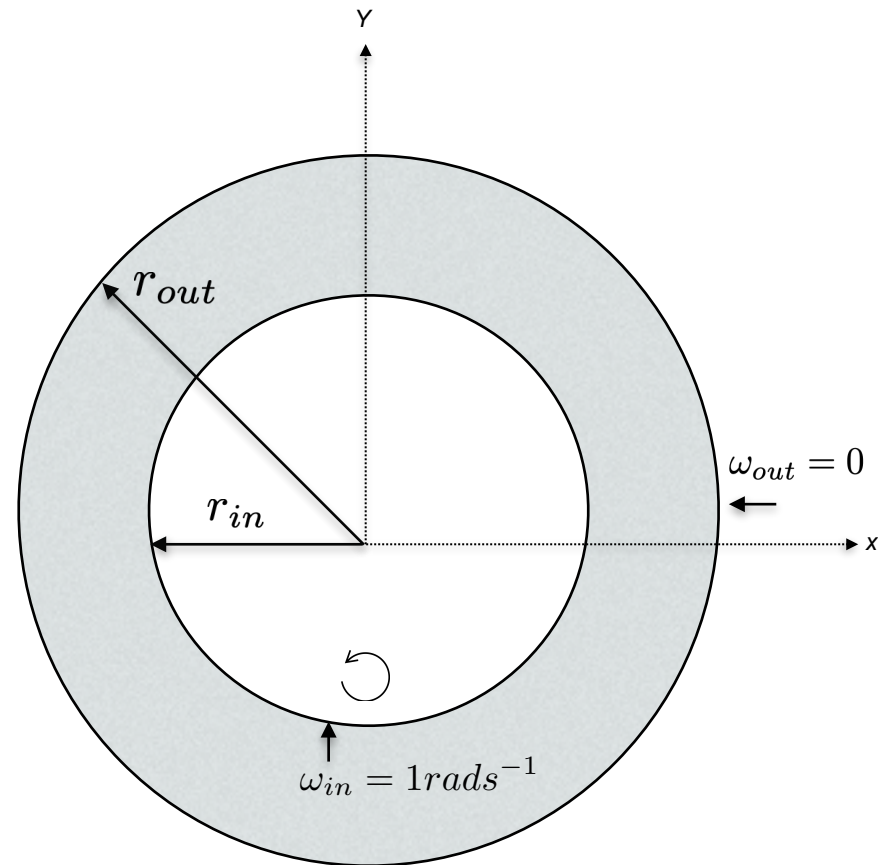
Continuous axial-Flow Couette device:

The material is sheared in the annulus between the interior and exterior cylinder shells of radii r_{in} and r_{out} respectively.

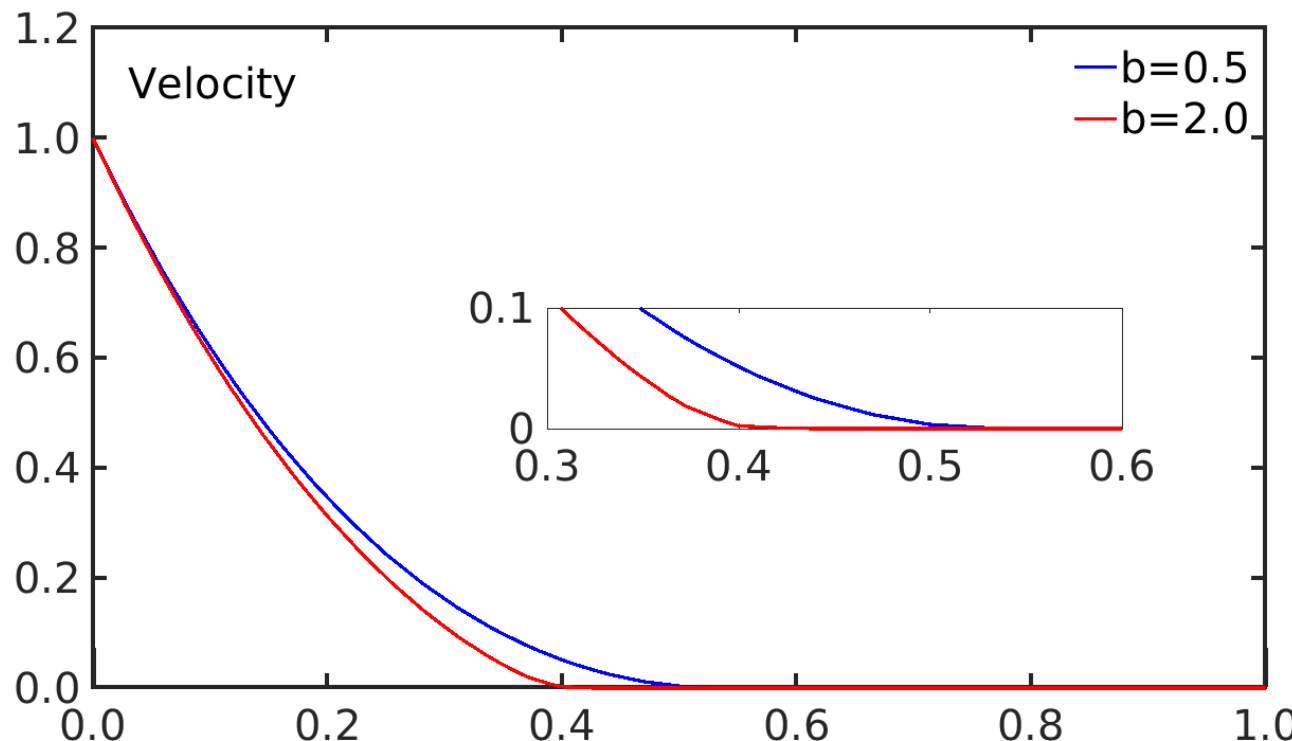
- ▶ Concentric cylinders
- ▶ Rotating inner cylinder with $\omega_{in} = 1 \text{ rads}^{-1}$
- ▶ Stationary outer cylinder
- ▶ Vertical flow super-imposed in radial direction

Investigations of thixo-viscoplastic phenomena

- ▶ Shear localization
- ▶ Shear banding
- ▶ Consistent transition points between velocity and structure

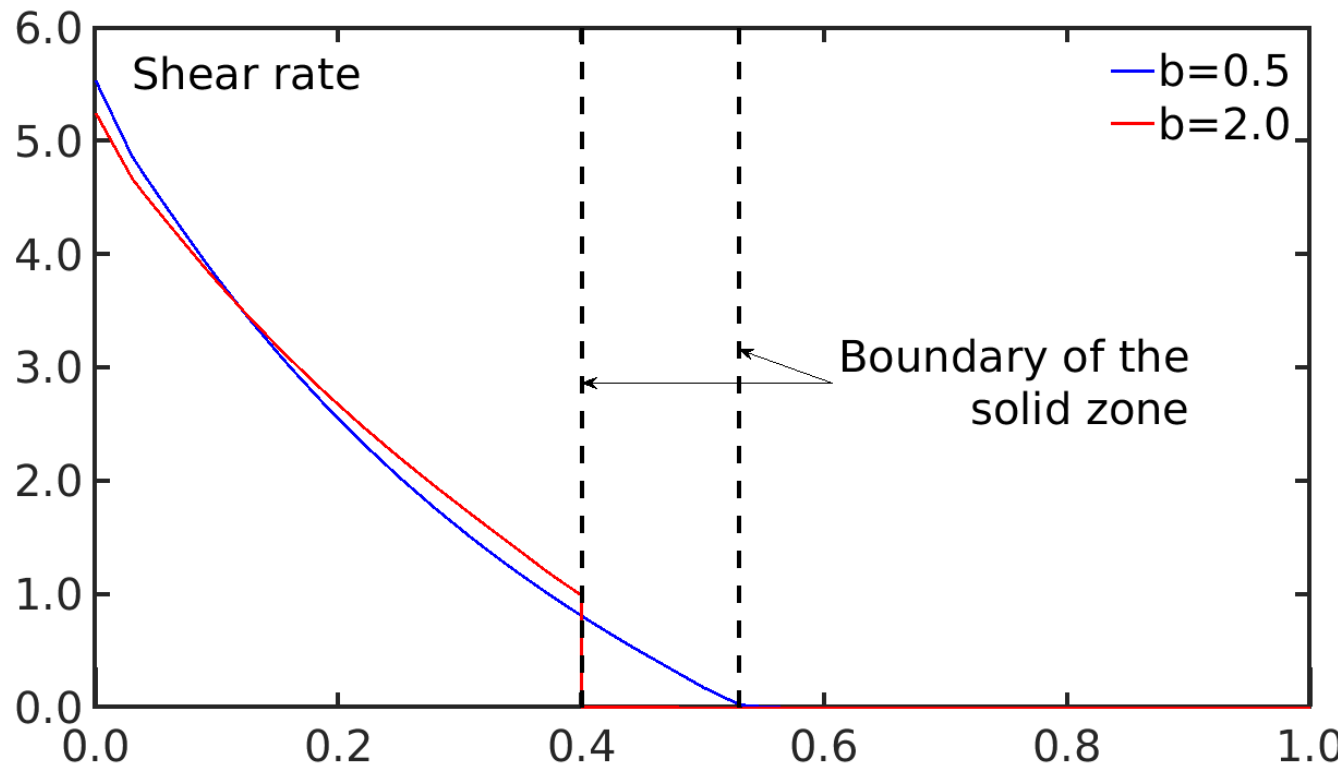


- Velocity profile at cut-line positions $c; c \in [0, 2\pi]$ in a Couette device w.r.t breakdown parameter



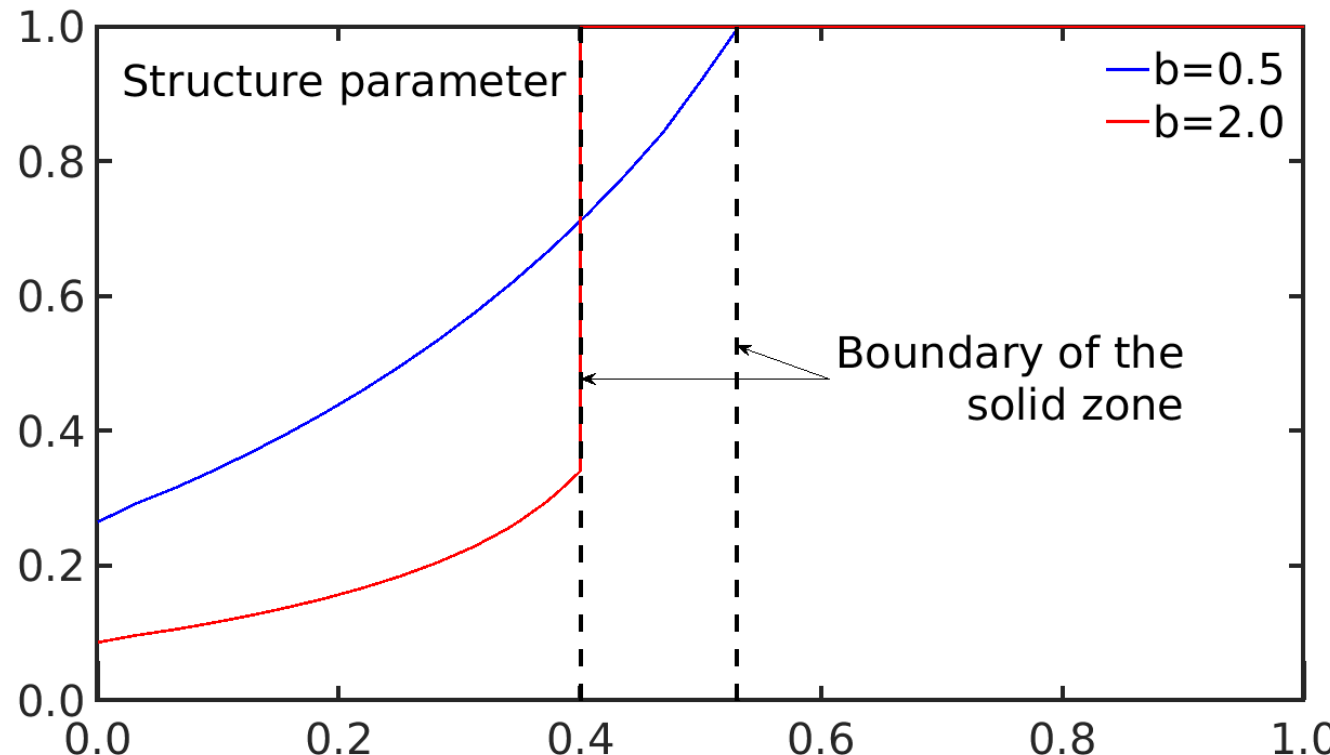
- ✓ Localization
- ✓ Shear banding

- Shear rate at cut-line positions $c; c \in [0, 2\pi]$ in a Couette device w.r.t breakdown parameter



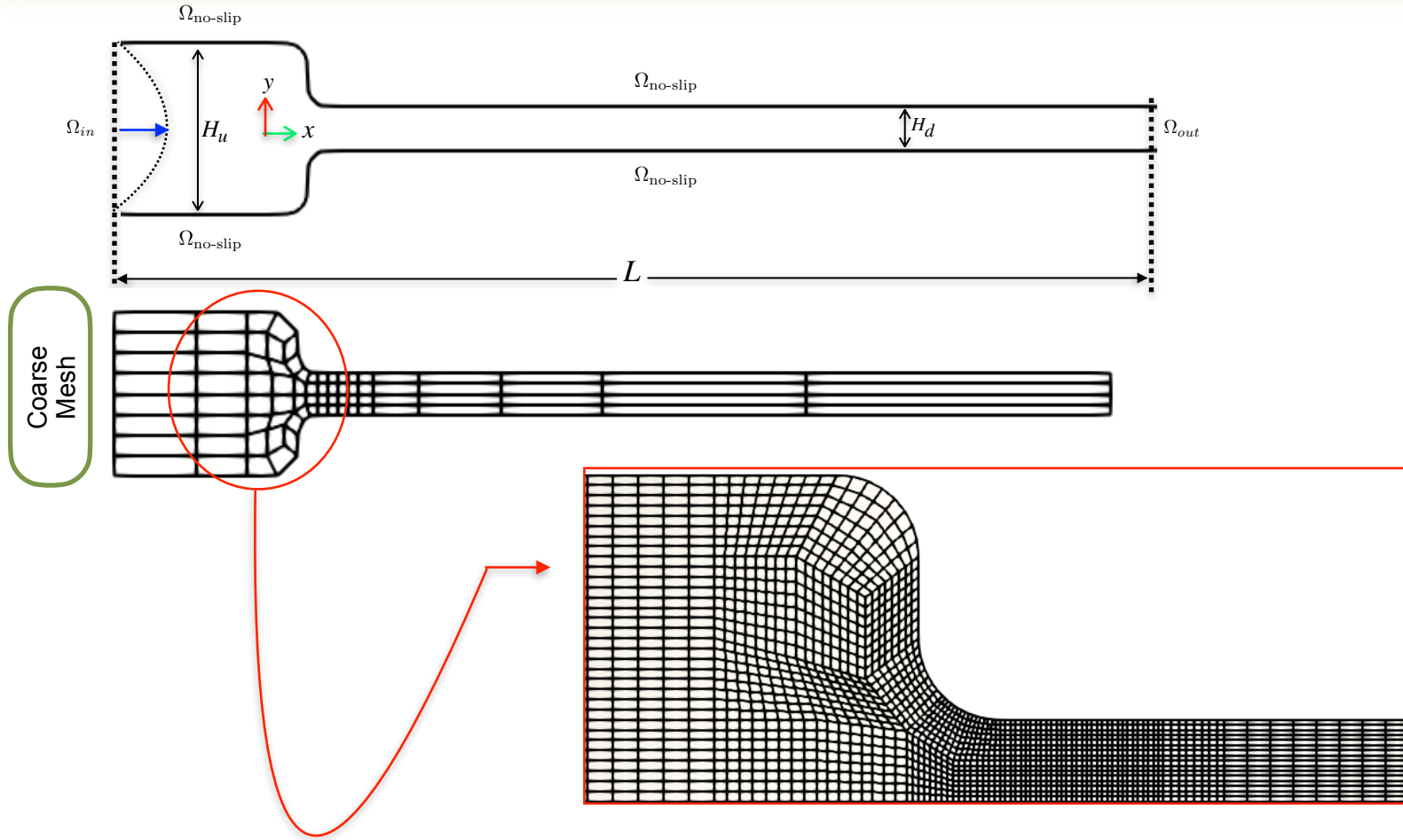
- ✓ Smooth and sharp transition are possible
- ✓ Transition point matches with the velocity

- Structure parameter at cut-line positions $c; c \in [0, 2\pi]$ in a couette w.r.t. breakdown parameter

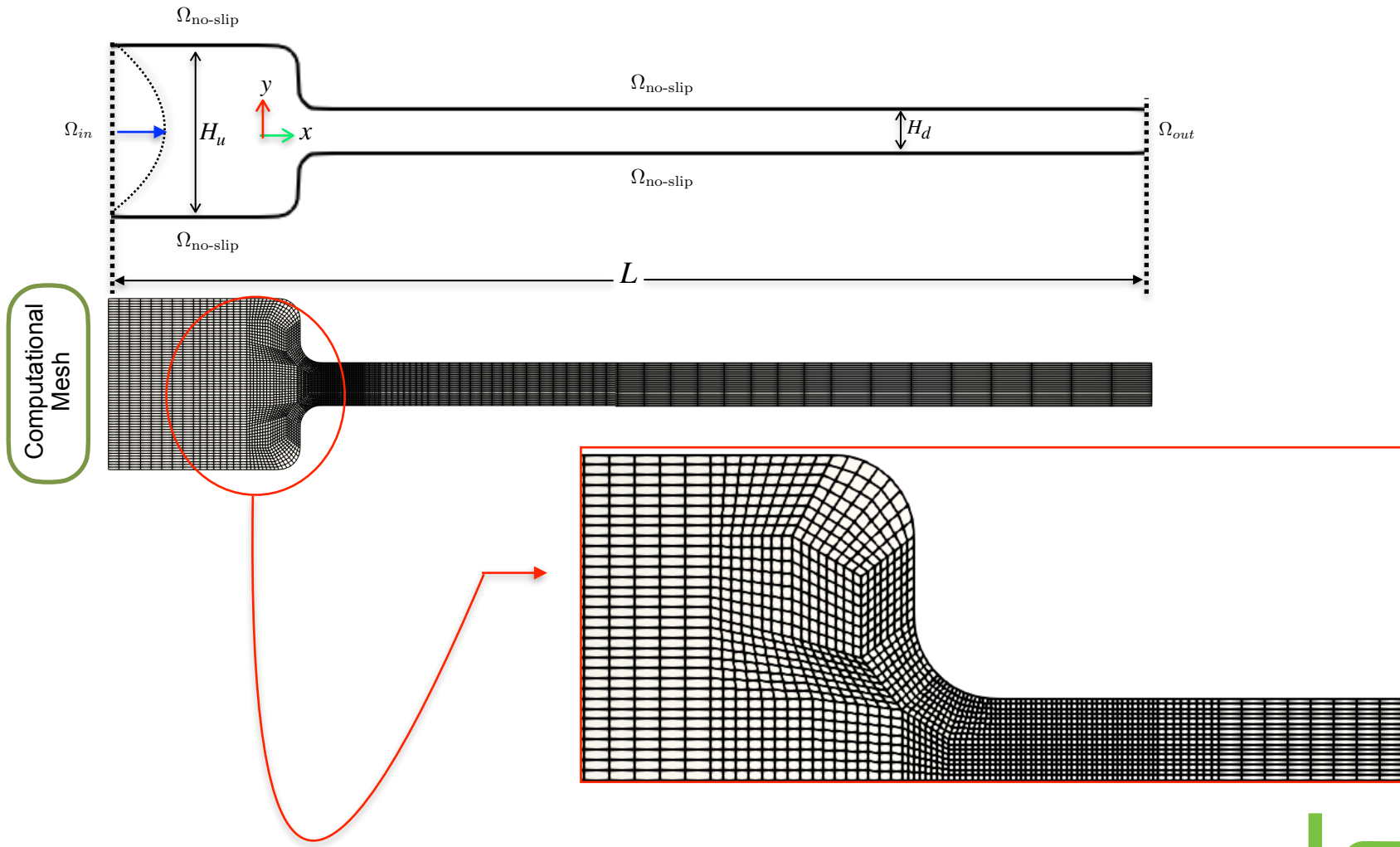


- ✓ Transition point matches with the velocity
- ✓ Structuring level is predicting shape and extent of rigid zones

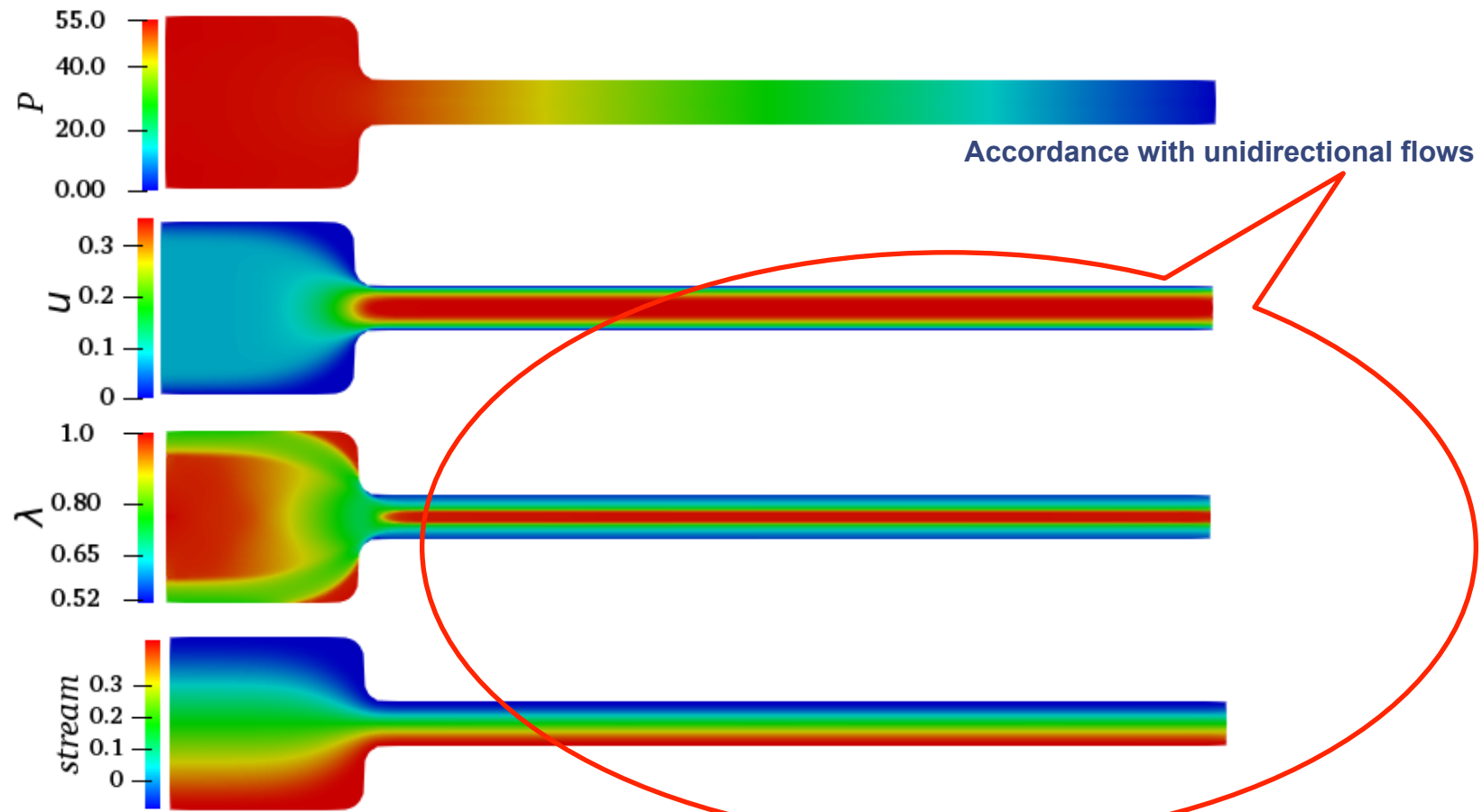
- 2D-FEM simulation results for thixo-viscoplastic flow- validation of 1D tool
- Specifying the “unidirectional profiles as boundary Data” in 2D for contraction



- 2D-FEM simulation results for thixotropic flow- validation of 1D tool
- Specifying the “1D-profiles as boundary Data” in 2D simulations for contraction domain

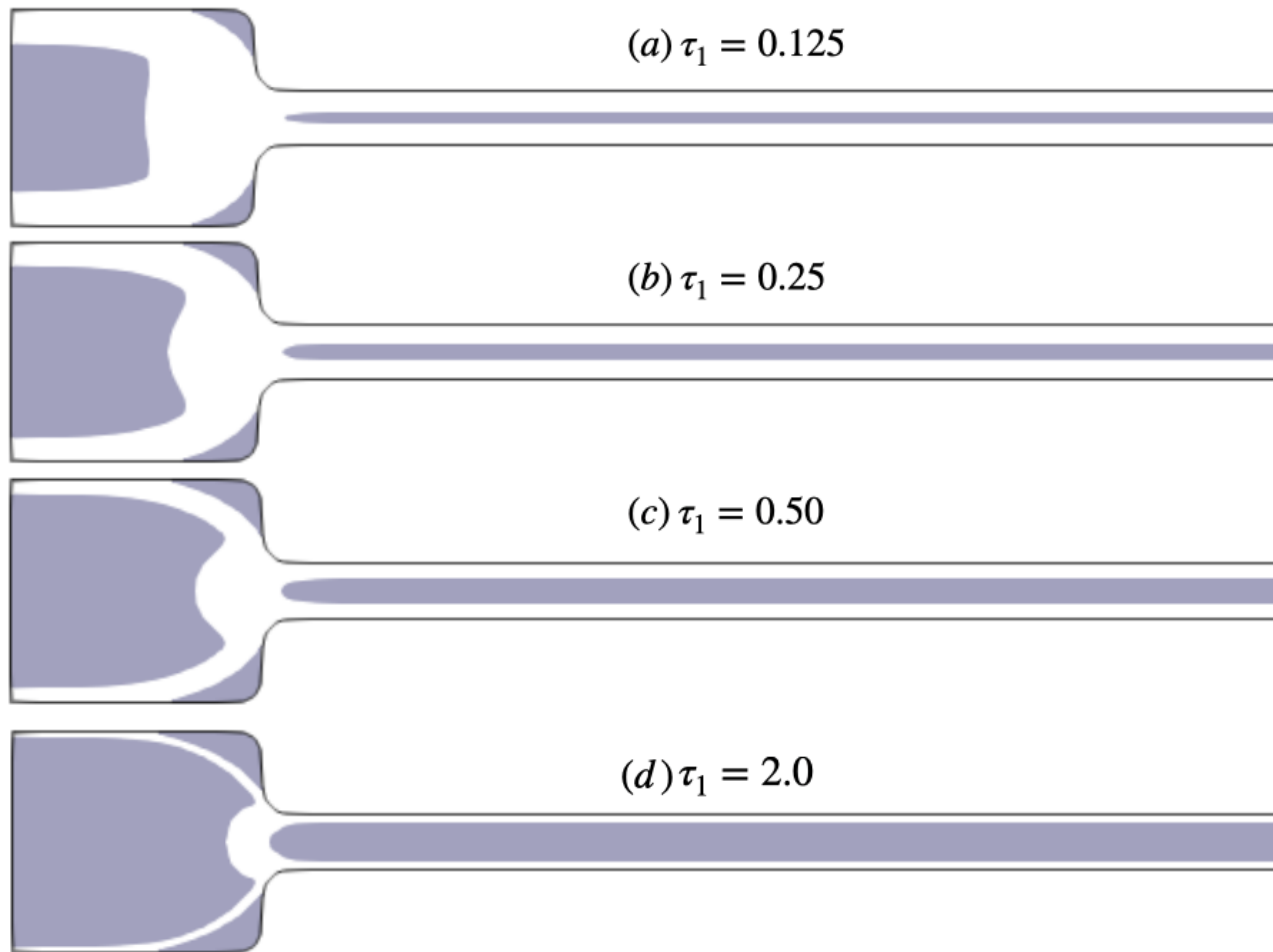


Contraction flow (smoothed)



- ✓ As predicted (u, λ, p) solutions
- ✓ Structuring level is predicting shape and extent of rigid zones

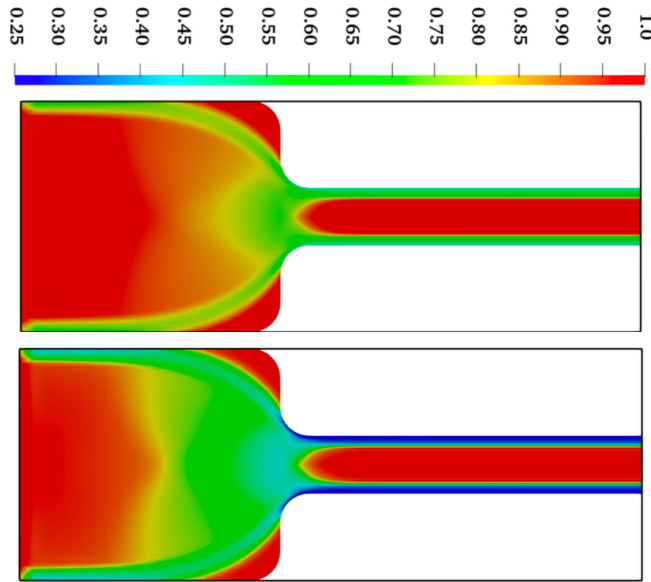
- progressive growth of unyielded zones (shaded)



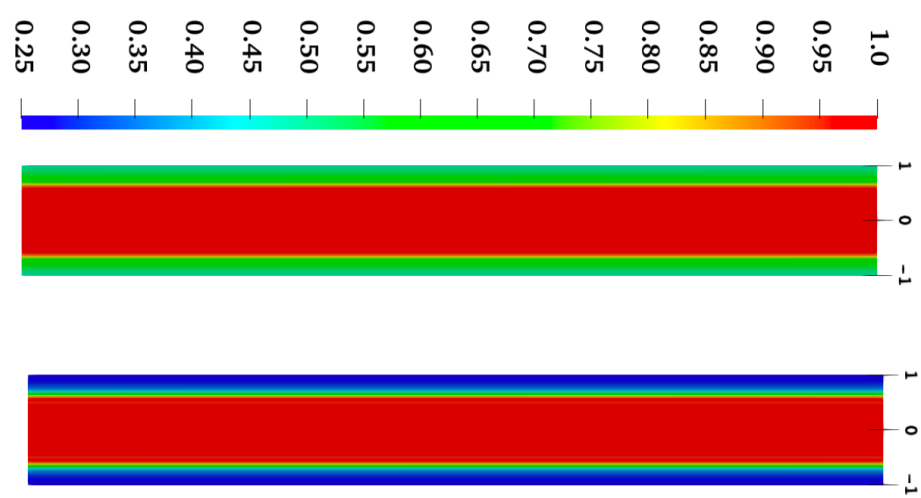
Unyielded zones in upstream and downstream are not merging

- Material micro-structural level w.r.t. breakdown

(i) Upstream channel & Entrance zone



(ii) Downstream channel



- Inherent thixotropy speed-up the breakdown

- ✓ Appearance of more breakdown layers
- ✓ Applications: restart pressure in pipelines should not be over-estimated

“Further investigation” regarding material structuring in thixo-elastoviscoplastic



An accurate, robust, and efficient numerical solver for TVP flows is developed using

- ✓ Higher order finite element method
- ✓ Monolithic Newton-multigrid
 - Adaptive discrete Newton's method with global convergent property
 - Geometric multigrid with local MPSC

To analyze the quasi-Newtonian model for TVP materials for different flow simulations

- ✓ Newtonian, VP, and TVP flow in Lid-driven cavity
- ✓ TVP flow in Couette devices
- ✓ TVP flow in curved contractions



1. Worrall, W. E. , Tuliani, S., Viscosity changes during the ageing of clay-water suspensions,*Transactions and journal of the British Ceramic Society*, **63**,167-185, 1964.
2. Coussot, P. Nguyen, Q. D. , Huynh, H. T. , Bonn,D., Viscosity bifurcation in thixotropic, yielding fluids, *Journal of Rheology*, **46 (3)**, 573-589, 2002.
3. Houska, M. , *Engineering aspects of the rheology of thixotropic liquids*. PhD thesis, Faculty of Mechanical Engineering, Czech Technical University of Prague, (1981).
4. Ashutosh Mujumdar, Antony N. Beris, Arthur B. Metzner, Transient phenomena in thixotropic systems, *Journal of Non-Newtonian Fluid Mechanics*, 102(2) ,157-178, 2002.
5. Gilmer R Burgos, Andreas N Alexandrou, Vladimir Entov, Thixotropic rheology of semisolid metal suspensions, *Journal of Materials Processing Technology*, **110(2)**, 164-176, 2001.
6. Dullaert, K. and Mewis, J. A Structural Kinetics Model for Thixotropy. *Journal of Non-Newtonian Fluid Mechanics*, **139**, 21-30, 2006.
7. Kheiripour Langrouri, M., Turek, S., Ouazzi, A., Tardos, G.I. An investigation of frictional and collisional powder flows using a unified constitutive equation, *Powder Technology*, **197**, 91-101, 2010.
8. Jenny, M., Kiesgen de Richter, S., Louvet, N., Skali-Lami, S. Dossmann, Y. ,Taylor-Couette instability in thixotropic yield stress fluids. *Phys. Rev. Fluids* (2017) **2**:023302–023323.
9. Ouazzi, A., Begum, N., Turek, S. Newton-multigrid FEM solver for the simulation of quasi-newtonian modeling of thixotropic flows. *Ergebnisberichte des Instituts für Angewandte Mathematik Nummer 635*, Fakultät für Mathematik,TU Dortmund University 638, 2021.
10. Turek, S., Ouazzi, A. Unified edge-oriented stabilization of nonconforming FEM for incompressible flow problems:Numerical investigations. *Journal of Numerical Mathematics* **15(4)**, 299-322, 2007
11. Burman, E., Stabilized Finite Element Methods for Nonsymmetric, Noncoercive, and Ill-Posed Problems. Part II: Hyperbolic Equations, *SIAM J. Sci. Comput.*, **36(4)**, A1911–A1936.
12. Kuzmin, D.; Löhner, R.; Turek, S. *Flux-Corrected Transport*, Scientific Computation, Springer, Subtitle: Principles, Algorithms and Applications, 3-540-23730-5, 2005.
13. Kuzmin, D.; Löhner, R.; Turek, S. *Flux-Corrected Transport*, Springer, 2nd edition, 978-94-077-4037-2, 2012
14. Ouazzi, A. *Finite Element Simulation of Nonlinear Fluids:Application to Granular Material and Powder*, Shaker Verlag Aachen, ISBN 3-8322-5201-0, 2006.

15. Ghia, U., Ghia, KN. and Shin, CT. High-resolutions for incompressible flows using Navier-Stokes equations and a multigrid method. *Journal of Computational Physics* **48**, 387–411, 1982.
16. Vanka, S. P., Block-implicit multigrid solution of Navier–Stokes equations in primitive variables, *Journal of Computational Physics* **65**, 138-158, 1986.
17. Botella, O. and Peyret, R. Benchmark spectral results on the lid-driven cavity flow. *Computers & Fluids* **27**, 421-433, 1998.
18. Bruneau, C. and Saad, M., The 2D lid-driven cavity problem revisited. *Computers & Fluids*, **35**, 326-348, 2006.
19. Schreiber, R. and Keller, HB. Driven cavity flows by efficient numerical techniques. *Journal of Computational Physics*, **49**, 310-333, 1983.
20. Goodrich, U. An unsteady time-asymptotic flow in the square driven cavity. In: IMACS 1st International Conference on Computational Physics, 1990.
21. Kupfferman, R. A central-difference scheme for a pure stream function formulation of incompressible viscous flow. *SIAM J. Sci. Comp.*, **23**, 2001.
22. Pan, TW. and Glowinski, R. A projection/wave-like equation method for the numerical simulation of incompressible viscous fluid flow modeled by the Navier-Stokes equations. *Comp Fluid Dyn. J.* **92** 2000.